MODELLING OF CESIUM CHEMISORPTION UNDER NUCLEAR POWER PLANT SEVERE ACCIDENT CONDITIONS

Miradji F. [*], Suzuki C., Nishioka S., Suzuki E., Nakajima K., Osaka M.
Japan Atomic Energy Agency
2-4 Shirakata, Tokai-mura, Naka-gun, Ibaraki-ken 319-1195, Japan
miradji.faoulat@jaea.go.jp; suzuki.chikashi@jaea.go.jp; nishioka.shunichiro@jaea.go.jp; suzuki.eriko@jaea.go.jp; nakajima.kunihisa@jaea.go.jp; ohsaka.masahiko@jaea.go.jp

Barrachin M.
Institut de Radioprotection et de Sureté Nucléaire,
PSN-RES, SAG, LETR 13115 Saint Paul Lez Durance, France.
marc.barrachin@irsn.fr

Do T.M.D., Murakami K., Suzuki M.
Nuclear System Safety Engineering
Nagaoka University of Technology
1603-1 Kamitomioka, Nagaoka, Niigata-ken 940-2188, Japan
maidung@vos.nagaokaut.ac.jp; murakami@vos.nagaokaut.ac.jp; suzuki_masahide@vos.nagaokaut.ac.jp

ABSTRACT

Towards the improvement of cesium (Cs) distribution in the Fukushima Daiichi nuclear power station (1F) by severe accident (SA) analysis codes, a series of work dedicated to the improvement of a model for Cs-chemisorption onto reactor stainless steel (SS304) structural material is reviewed. Experimental tests to identify the influencing chemical factors on the Cs chemisorption were first given. It was found that the surface reaction rate constants which correspond to the Cs chemisorbed amount were influenced by not only temperature but also atmosphere (H_2/H_2O), cesium hydroxide (CsOH) concentration in the gas phase and silicon (Si) content in SS304. Important chemical factors revealed were implemented into an improved Cs chemisorption model, which allowed great reduction of the uncertainties. Further improvement for implementing the revaporization effect of the Cs chemisorbed species was made by thermodynamic considerations. Another series of studies were undertaken for this purpose to consolidate and extend the knowledge on the thermodynamic properties of likely formed Cs chemisorbed species in SA conditions. A literature review was conducted to assess the availability of such properties, accompanied by an illustration of those implemented in the database Mephista currently developed at IRSN. The review revealed the necessity of consolidation and extension of Cs-(Fe)-Si-O system onto the current database. Accordingly, a Density Functional Theory (DFT) based methodology was developed for the preparation of thermodynamic properties of possible Cs chemisorbed species. The DFT computed vibrational frequencies were compared to Raman spectroscopy, revealing a coherent matching between the calculated and measured vibrational peaks. The existing Cs-(Fe)-Si-O thermodynamic properties were found to be in good agreement with both DFT computed values and our newly performed experimental measurement results. The unknown properties of identified Cs chemisorbed species were finally elucidated by the DFT based methodology.

[*]: Corresponding author
Email address: miradji.faoulat@jaea.go.jp

KEYWORDS
Cesium, Chemisorption, Modelling, LWR SA

1. INTRODUCTION

Following the severe accident (SA) of Fukushima Daiichi Nuclear Power Plant Station (1-F), the evaluation of fission products (FP) distribution is of crucial importance for the debris-retrieval and decommissioning work. Particular attention is paid to radioactive cesium (Cs) nuclides ^{137}Cs since the released Cs from the damaged fuel not only released into the environment due to its volatile feature [1] but also would interact with reactor structural materials to retain on their surfaces [2]. Such Cs retention would give rise to the radiation exposure of the workers for the decommissioning of 1-F [1]. The SA analysis code is a candidate as a prediction tool for the Cs distribution inside the reactor, as well as that for the released amount to the environment. Regarding the analyses on the 1-F SA by several SA analysis codes, the results for Cs distribution have shown large discrepancies each other. In particular, the divergence was larger for Cs retention at the upper part of the reactor pressure vessel (RPV) [3]. It was stated that Cs retention there is mainly due to Cs chemisorption onto the reactor structural material (stainless steel).

The Cs chemisorption mechanism had been investigated after the SA of Three Mile Island 2 nuclear power plants mainly by laboratory studies in the USA and European countries [4-8]. $CsOH_{(g)}$ is considered as the main cesium source for chemisorption tests. Indeed, albeit that thermodynamic equilibrium calculations predicted that CsOH and CsI were the main released cesium gaseous species from fuel [9], experiments performed by Elrick and Powers [6] showed that the chemisorption rate between CsI and the SS surfaces was very low. The cross section analysis did not reveal any Cs diffusion into the inward layers of the SS samples. Regarding the possible effect of Cs_2MoO_4 as Cs source, we did perform fundamental tests [10] revealing that Cs_2MoO_4 might be formed by CsOH chemisorption on SS type 316, in which Mo is included as a component element. Thus, Cs_2MoO_4 chemisorption on SS304 is considered extremely difficult to occur, corroborated by the fact that partial pressure of Cs_2MoO_4 in high temperature is very low (about 0.05 $\mu g.cc^{-1}$) when using Yamawaki et.al [11] equation of vapor pressure of Cs_2MoO_4. As we performed Cs chemisorption tests with CsOH concentration of 0.23 to 19.86 $\mu g.cc^{-1}$, thus Cs chemisorbed amounts can be much lower in the case of Cs_2MoO_4 as initial source of Cs.

The Cs chemisorption models established through past studies [4-8] are considered one of the main cause of discrepancies among the analyses by SA analysis codes, as the models are insufficient to cover the various chemical factors appeared along with 1-F SA progressions in the several 1-F units [12].
In line with our work on the construction of FP chemistry database [13], this paper is intended to provide a review for a series of the Cs chemisorption modelling work. Obtained results and established methodology through this work can be reflected in consolidation and extension of knowledge for high-temperature FP chemical behaviors inside the reactor, which can consequently contribute to the enlargement of the FP chemistry database.

The next section introduces our fundamental research [14] to improve the implemented Cs chemisorption modelling in SA analysis codes, mainly by investigating experimentally the surface reaction rate of Cs chemisorption onto SS specimens. The boundary conditions set experimentally for $CsOH_{(g)}$ concentration, atmosphere (H_2/H_2O ratio) and temperature first aimed to reproduce the previous existing chemisorption tests [4-8], in order to assess the reliability of existing Cs chemisorption models. Secondly, as we aimed to accumulate data for the 1-F SA Cs chemisorption mechanisms, the experimental conditions were set according to the results of 1-F SA analysis by MAAP code[12], which established a temperature range around 700-1000 K for RPV region, an oxygen ratio between $p(H_2)/p(H_2O)$ of 0.25-0.50. In-core release

time was determined to last from 3 to 6 hours. The initial concentration of CsOH deduced by the molar ratio of Cs element, led to 500g.m^{-3}.

Elrick and Powers [6] showed that a prior oxidation to cesium release had little impact on Cs chemisorption process. Indeed, there was not significant difference in the Cs amounts between as-received and pre-oxidized SS coupons. The SS specimens presented an outer layer rich of iron oxide and an inner layer with spinel chromates [6], in agreement with the SS oxide layers identified in our tests [10,14,15]. Moreover, it was observed that the nature of the oxide layers might vary with the atmosphere, and their thickness with increasing temperature [16], both parameters were studied in our tests.

On the basis of our experimental investigations which underlined significant influences of several chemical factors such as atmosphere, $CsOH_{(g)}$ concentration and Si content in the SS specimen for the Cs chemisorption process, the improvement of Cs chemisorption model by Nakajima *et al.* [17] is then described. A mass transfer type model was developed to describe the surface reaction rate of Cs chemisorbed amount referred to as water-soluble and water-insoluble. In this paper, only the water-insoluble Cs amount model is presented, as it might be the main source of radiation exposure in the case of 1-F dismantling and decommissioning work.

The third section presents the work dedicated to consolidate and extend knowledge on the thermodynamic properties of Cs chemisorbed species, which allows implementing the atmospheric influence on the Cs chemisorption modelling by including the revaporization phase of Cs chemisorbed species. A literature survey is first provided to analyze the status of thermodynamic properties of Cs chemisorbed species available in the literature and their implementation in the European thermodynamic database Mephista, currently developed at IRSN [18]. Then, the properties of possible Cs chemisorbed species identified in our study are determined by a Density Functional Theory (DFT) based methodology [19, 20]. The accuracy of computed values is discussed not only within the literature references, but also by comparison with our recent experimental studies. These are also aiming to characterize the mainly identified Cs chemisorbed species $CsFeSiO_4$ by Raman spectra [21] and $Cs_2Si_4O_9$ by low temperature heat capacity measurements [22]. Finally, an application of the enhanced Cs chemisorption model is given to have more insight into the revaporization process of likely formed Cs chemisorbed species.

2. INVESTIGATION OF CESIUM CHEMISORPTION MECHANISM

To grasp the phenomenology of Cs chemisorption process, we conducted fundamental tests of CsOH chemisorption onto stainless steel specimen in both reducing and oxidizing environment. The tests aimed first to assess the reliability of existing chemisorption models (referred to hereafter as Bowsher's model [7]), which highlighted the influence of temperature. In our study, we focused on high and medium temperature range and selected representative temperatures points in those ranges. To obtain new experimental data in an environment similar to those of 1-F SA [12], we performed tests with higher CsOH concentration than reported on past laboratory studies. In addition, the Si content in SS specimen was varied to highlight the nature of the Cs chemisorbed species. The influence of these several experimental boundary conditions, referred hereafter as chemical factors, was discussed by calculating the surface reaction rate constant v_d for water-soluble and water-insoluble Cs formed species. The reaction rate constant equation, used to obtain the surface reaction rate from experimental measurements is defined as follows:

$$N = \frac{1}{A}\frac{dM_d}{dt} = v_d C_g \quad (1)$$

where N is the absorption rate of Cs per unit time unit area [μgCs/cm^2.s^{-1}], and M_d the Cs-deposition amount [μg], A is the surface area of the SS304 specimen [cm^2], t is the heating time [s], v_d the surface reaction rate constant [cm.s^{-1}], and C_g the concentration of CsOH in the gas phase [μg CsOH.cm^{-3}]. The following paragraphs present the results of the experimental tests conducted to determine the surface reaction rate v_d and the influence of chemical factors. Then, the analysis of the obtained results through

comparison within the existing chemisorption modelling and its improvement to represent our experimental results are provided.

2.1. Cs chemisorption tests

To obtain representative results for both assessments of Cs chemisorption models and 1-F conditions, several tests were performed within the temperature range from 873 to 1273 K. The SS specimens were SUS304L type (referred hereafter by SS304)-based ones with the composition of chromium (Cr): 19.37~19.48 wt%, carbon (C): 0.03 wt%, nickel (Ni):8.75~8.97 wt%, silicon (Si): varying from 0.1 to 4.9 wt%, and iron (Fe): from 70 to 65 wt%. A CsOH concentration in the gas phase of 0.23 to 19.86 $\mu g.cm^{-3}$ was used. The schematic illustration of the experimental apparatus CREST (Chemical REaction with STeel) is presented in Fig. 1. Details about the experimental set-up could be found in our previous studies [10, 14,15].

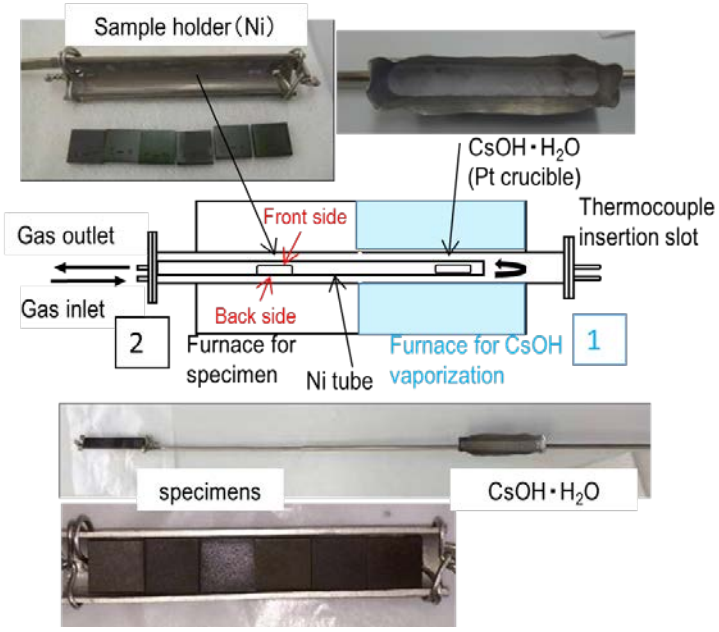

Figure 1. Illustration of CREST apparatus [14].

As shown in Fig. 1, the CREST facility is constituted of two furnaces. The furnace number (1) enables to vaporize the anhydrous CsOH powder from the Pt crucible, at 920.15 K for achieving online control of CsOH concentration with the temperature [14]. Then, in the furnace for specimen (number 2), the CsOH vapors are transported inside a Ni tube to react with the SS specimens at a given temperature (from 873 to 1273 K). The post analyses following the chemisorption tests were conducted by XRD and SEM/EDX to characterize the morphology and elemental distribution of deposits on the surface and the oxidized layer. Then, leaching tests of the Cs chemisorbed specimens were conducted by using two kinds of leachants to separate the water-soluble and -insoluble Cs species since the surface reaction rates were determined individually for them. Finally, ICP-MS analyses were performed for the determination of the water-soluble and -insoluble Cs amounts for the calculation of the surface reaction rates. Details on samples analysis can be found in elsewhere [10, 14, 15]. The main results regarding the influence of the chemical factors, i.e. the temperature, atmosphere, Si content in SS and CsOH concentration, are summarized in next subsections.

2.1.1. Influence of temperature and atmosphere

The surface reaction rate obtained in our tests for the water-soluble Cs amount did not present significant differences with Bowsher's study regarding the impact of temperature [10]. Indeed, in both studies, the

amount of Cs decreased with increasing temperature, regardless of the atmosphere. The reaction rates of the water-insoluble Cs compounds are compared to those of Bowsher's study in Fig. 2. It can be seen from our results that the reaction rate of water-insoluble Cs compounds decreased with increasing temperature in Ar-H_2 reducing atmosphere, indicating a possible revaporization of Cs chemisorbed species at the higher temperature. Such observation agrees with that by the study of Bottomley *et al*. [2]. In their study, it is found that the maximum revaporization rate of Cs was attained in Ar-H_2 atmosphere, while steam or steam-H_2 environment presented a much lower revaporisation rate of Cs. However, in Bowsher's study [7], the water-insoluble Cs amount increased proportionally to the temperature in reducing atmosphere. These results might be caused by a different atmosphere between Bowsher's and Nishioka's studies. By contrast, in oxidizing atmosphere, amount of Cs chemisorbed species increased at higher temperatures in both Bowsher's and Nishioka's experiments [14]. Thus, it can be said that the atmosphere significantly influences the Cs chemisorption features and should be taken into account into the Cs chemisorption modelling. The difference of temperature was resulted not only in the different morphologies of Cs chemisorbed spe-

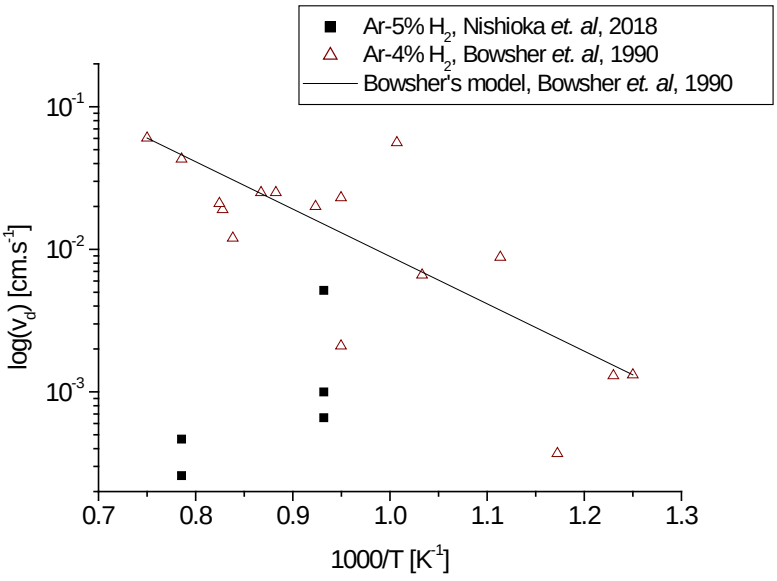

(a)reducing atmosphere

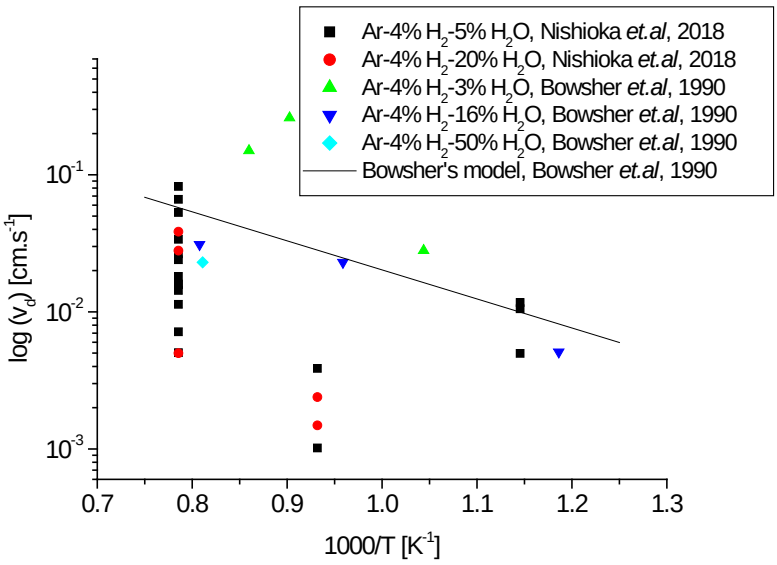

(b) oxidising atmosphere

Figure 2. Temperature and atmosphere dependences of surface reaction rate constant v_d of water-insoluble Cs. (a) reducing atmosphere; (b) oxidizing atmosphere, extract from [14]. The average deviation of v_d is ±34,7%.

-cies but also the chemical speciation. Namely, Cs ferrates were identified at temperature region around 873 K, whereas Cs silicates (Cs-(Fe)-Si-O) above 1073 K [18-20]. The change of the chemisorption mechanism is highlighted in Fig. 2 (b) where a minimum is reached at c.a. 1100 K for the water-insoluble Cs species surface reaction rate in Ar 45%H_2-5%H_2O atmosphere. A more detailed discussion regarding the change of speciation is provided in the next subsection.

2.1.2. Si content in SS and CsOH concentration in gas phase.

Illustrations of v_d variation in function of Si contents are provided in Appendix A.
The results in Fig. A (a) indicated no dependence of Si contents for water-soluble Cs species. It was stated that the chemical form of these species were not Cs silicates. The amount of water-insoluble Cs species onto the SS304 specimen increased with Si content at high temperature (1073 and 1273 K), as portrayed by the increasing surface reaction rate in Fig. A (b), but did not vary for 873 K, reflecting the discussion in the above subsection about the influence of temperature on identified Cs chemisorbed species. Fig. 3 presents the analysis of Cs chemisorbed species onto SS304 specimen, showing both the Cs silicates (Fig. 3(a)) and Cs ferrates (Fig. 3 (b)).

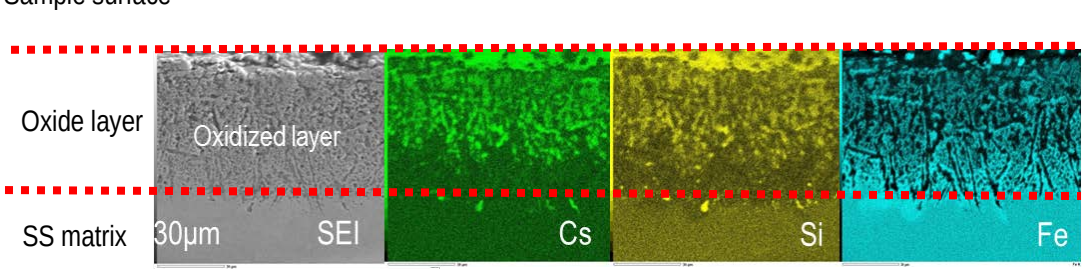

(a) Elemental distribution of the cross section in the SS304 specimen at 1273 K, within Ar-5%H_2O-5%H_2 atmosphere and 1.0 wt% Si content.

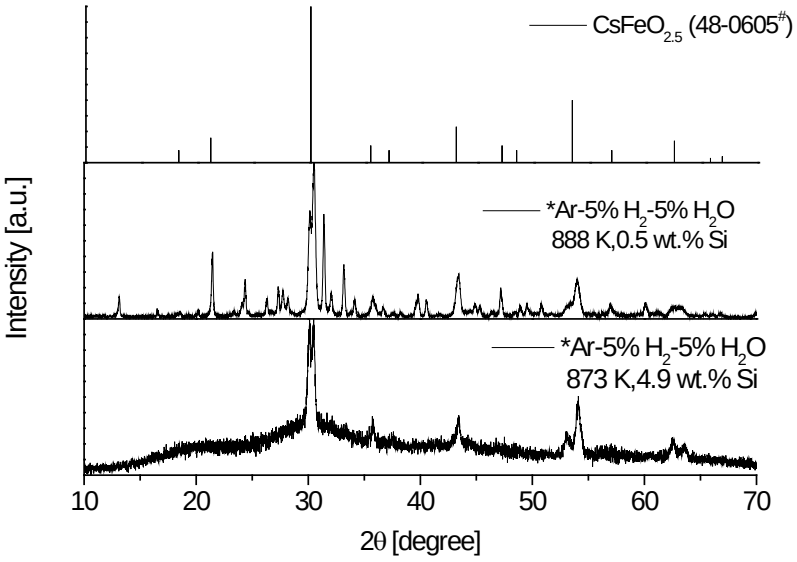

(b) XRD patterns of the SS304 specimens after the chemisorption test around 873 K in the H_2O-containing atmosphere. * From Nishioka *et al.* study [14], # from JCPDS-ICDD database.

Figure 3. Identified Cs water-insoluble species: (a) Cs silicates (iron containing), (b) Cs ferrates.

The influence of Si content appeared significant especially for the high-temperature region and should be reflected onto the Cs chemisorption modelling.

Illustrations of the evolution of surface reaction rate constant in function of CsOH concentration is provided in Appendix B Fig. B(a) and (b) for water-soluble and -insoluble Cs species, respectively.
Fig. B (a) underlined that with 1wt.% Si content in the SS304 specimen, the surface reaction rate of water-soluble Cs increased at higher CsOH concentration in the range of investigated high temperature. Oppositely, for water-insoluble Cs species, Fig. B (b) shows that the surface reaction rate decreased continuously at higher CsOH concentration. Such behavior should, therefore, be reflected in the modelling of Cs chemisorption process by implementing a surface reaction rate equation dependent on CsOH concentration.

2.2. Cs chemisorption modelling

As reported by Nakajima *et al*. [17], the use of Bowsher's model [7] to represent our surface reaction rate leads to large scattering of the experimental data along the modelled ones. Thus, to improve the model requires consideration of not only temperature but also the chemical factors such as CsOH concentration, Si content in SS304 and so on as discussed in the previous section. A mass transfer type model was used as the modified Cs chemisorption model for this purpose. The developed Cs chemisorption model allows implementing CsOH concentration in the gas phase (C_g) and Si content in SS specimen (C_B), using a penetration theory [25], as illustrated in Fig. 4, based on a mass action law at the gas solid-interface. Consequently, the improved model presented in Eq. 2 was obtained [17].

$$v_d = \frac{7.027 \pm 2.794}{C_g^{\,0.5225 \pm 0.0597}} \sqrt{C_B}\, exp\left(-\frac{6552 \pm 1197}{T}\right) \quad (2)$$

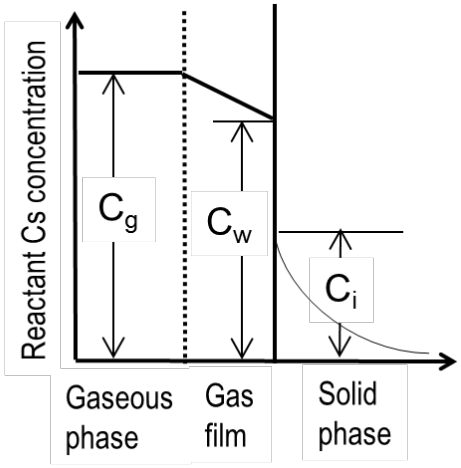

Figure 4. Illustration of the penetration image around the gas-solid interface. C_g is the initial CsOH concentration, C_w the concentration of Cs reactive species at the interface between the gas phase and solid phase (gas film), C_i the concentration of Cs reactant species in the solid phase at the interface [17].

The coefficients in Eq. 2 were determined from the regression analysis of the experimental v_d. The results of the calculated v_d presented in the study by Nakajima *et al.* [17] are illustrated in Fig. 5 for water-insoluble Cs amount in the oxidizing atmosphere.

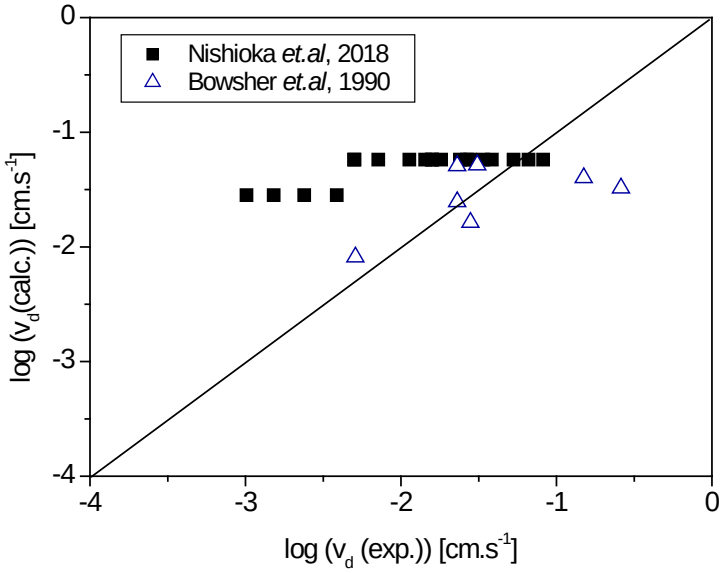

(a)

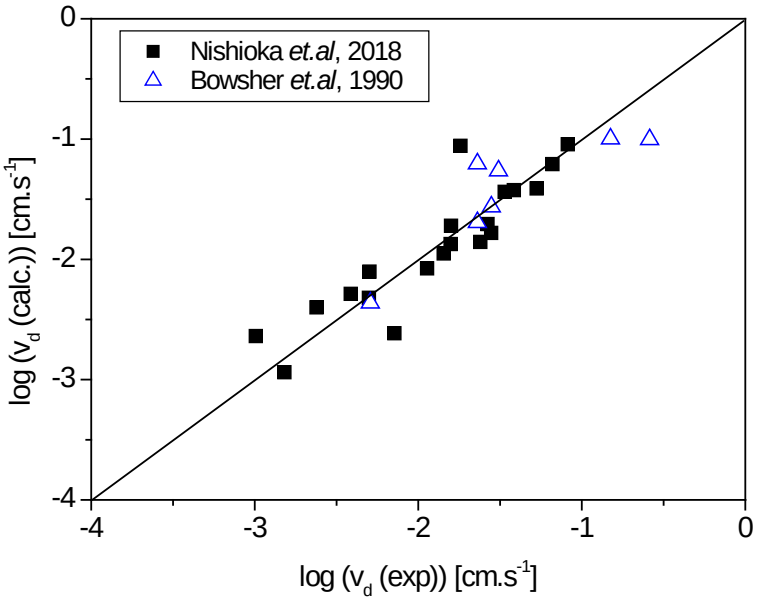

(b)

Figure 5. Comparison of the calculated v_d with the experimental v_d, (a) calculated by the existing model [7]; (b) calculated by the improved model [17].

It could be noticed in Fig.5 (b) that with the improved Cs chemisorption model a much better agreement was achieved. Two-fold standard deviations 2σ are 0.53 and 1.43 respectively for the improved and existing model, which corresponds to the improvement of more than one order of magnitude [17].

In order to take into account atmosphere influence onto Cs chemisorption modelling, the inclusion of revaporization phase of Cs chemisorbed species is considered.
The rate of revaporized Cs from water-insoluble Cs species could be expressed by using the equilibrium vapor pressures of the Cs species *i* revaporized from the chemisorbed cesium silicate compounds, p_i. Thus, the revaporization rate could be described as follows:

$$N_R = \sum_i k_{g_i}(C_{w_i} - C_{g_i}) \tag{3}$$

and

$$C_{w_i} = \frac{p_i}{R\,T} \tag{4}$$

where N_R is the revaporization rate of Cs, k_{g_i} the mass transfer coefficient of the re-vaporized Cs species *i* in the gas phase, C_{w_i} the concentration of the re-vaporized Cs vapor species *i* at the SS surface, C_{gi} the concentration of the re-vaporized Cs species *i* in the bulk gas stream, *R* the gas constant and *T* the absolute temperature. In this model, revaporization would occur when C_{w_i} is higher than C_{gi}. The vapor pressure of Cs chemisorbed species *i* could be obtained from their thermodynamic properties.
The next section discusses the availability of such thermodynamic properties for the Cs chemisorbed substances under the LWR SA conditions, in particular, those of 1-F severe accident.

3. THERMODYNAMIC PROPERTIES OF Cs CHEMISORBDED SPECIES

To take into account the revaporization phase of Cs in the chemisorption modelling, we have investigated the possible formed Cs-(Fe)-Si-O substances and their thermodynamic properties. As a first step, a literature review, as well as the contents of the Mephista database currently developed at IRSN [18] is provided to underline the available data for Cs chemisorbed species onto SS surfaces. We will show that the available experimental data is rather poor. Consequently, in a second step, the thermodynamic properties of likely formed Cs chemisorbed species were determined by a DFT based methodology [19,20]. They are detailed and assessed within available literature references and our recently performed experiments to characterize $CsFeSiO_4$ Raman spectra [21] and measured low-temperature heat capacity of $Cs_2Si_4O_9$ [22]. Finally, the possible revaporization of major characterized Cs chemisorbed species in our experiments is estimated using the constructed Cs chemisorption modelling.

3.1. Availability of thermodynamic properties of Cs chemisorbed species.

So far, several structurally characterized cesium silicates have been reported in the Cs_2O-SiO_2 pseudo-binary section, i.e. from the cesium oxide rich-part to the silica-rich part $Cs_6Si_2O_7$ ($3Cs_2O.2SiO_2$) [26], Cs_2SiO_3 ($Cs_2O.SiO_2$) [26], $Cs_8Si_6O_{16}$ ($4Cs_2O.6SiO_2$) [27], $Cs_2Si_2O_5$ ($1Cs_2O.2SiO_2$) [28], $Cs_6Si_{10}O_{23}$ ($3Cs_2O.10SiO_2$) [29, 30], and $Cs_2Si_4O_9$ ($1Cs_2O.4SiO_2$). Another compound outside the pseudo-binary section, $Cs_{10}Si_7O_9$ is reported by Hoffmann [31]. We can notice that the $Cs_2Si_4O_9$ structure is not properly known. The Cs_2SiO_3, $Cs_2Si_2O_5$, $Cs_2Si_4O_9$, and $Cs_6Si_{10}O_{23}$ compounds are indicated to melt congruently at 1100 K [32], in the range 1343-1369 K [33-36], 1223 K [33], and 1208 K [29] respectively. The available measurements related to thermodynamic properties of the different cesium silicate compounds are reported in Table I. Most of them are not known and only estimated in the NPL report in 1973 [32] even if some experimental data are available, mainly for the richest-silica oxide compound, $Cs_2Si_4O_9$, coming from Cordfunke [37], Boivin [34] and Ball [38]. For this compound, the standard enthalpy of formation has been measured by dissolution calorimetry as well as the heat increment.

The Cs_2O-SiO_2 system was partially investigated by Alekseeva [33], in the composition domain of Cs_2O mole fractions less than 0.45. She only put in evidence two stoichiometric compounds in the SiO_2-rich part, $Cs_2Si_4O_9$ and $Cs_2Si_2O_5$, but did not mention the silica-richest ones, $Cs_6Si_{10}O_{23}$ and $Cs_8Si_6O_{16}$. In the studied composition range, there is no indication of liquid immiscibility, also confirmed by Charles [39], but the presence of two eutectic transformations, between pure silica and $Cs_2Si_4O_9$ at 1148 K and between $Cs_2Si_4O_9$ and $Cs_2Si_2O_5$ at 1183 K. The liquidus temperatures were determined mainly by examination of samples quenched from high temperature. The liquid phase properties were more recently investigated with measurements of relative partial molar enthalpies, of SiO_2 in SiO_2–Cs_2O by drop-solution calorimetry at 1465 K [40].

In the Mephista thermodynamic non-ideal solution database currently developed at IRSN which contains the following elements O-Pu-U-Zr-Fe-Si-C-Cs-Mo-La-Ba-Ru-Sr-Ce+(H, Ar), the binary systems, Cs-O, Cs-Si, Si-O are modelled within the Calphad approach. Considering the lack of data especially in the rich-cesium oxide region, the Cs_2O-SiO_2 pseudo-binary section is not modelled in Mephista. Only the ternary compounds Cs_2SiO_3, $Cs_2Si_2O_5$, and $Cs_2Si_4O_9$ are considered, with their respective thermodynamic properties taken in Barin [41], not far from the estimated data from Spencer (Table I).

The literature survey of available thermodynamic properties suggests a consolidation of existing data. An extension of the database to implement possible Cs-Fe-Si-O chemisorbed species appears also necessary in order to take into account the actual chemical environment related to the 1-F SA.
The next section presents the consolidation and extension of Cs chemisorbed species thermodynamic properties from a DFT based methodology.

Table I. Available thermodynamic properties implemented for Cs-Si-O system in Mephista database compared with literature.

Properties	$\Delta_f H°_{298.15\ K}$	$H_T-H_{298.15\ K}$	$S_{298.15K}$	$\Delta_{fus}H$	T_{fus}	[Ref.]
	kJ.mol-1	T range (K)	$J.K^{-1}mol^{-1}$	kJ.mol-1	K	Year
Cs_2SiO_3	-1558.3*	-	176.6	39.7*	1100*	[32]1973
	-1528	310-800	175.7	39.7	1100	**Mephista**
$Cs_2Si_2O_5$	-2460.9*	-	209.2*	52.3*	1343	[32]1973
		-	-	49(5)	1369(5)	[37,38]1993
	-2461	-	209.2	52.3	1343	**Mephista**
$Cs_2Si_4O_9$	-4341.1*		313*	43.9*	1223	[32]1973
	-4297.6(5.4)	475-825	313*			[37,38]1993
	-4307.6		292.9	43.9	1223	**Mephista**
$Cs_2Si_{10}O_{23}$	-	-	-	156(159)	1208(1)	[29] 2008

**: estimated value, (): uncertainties*

3.2. Thermodynamic properties of Cs-(Fe)-Si-O chemisorbed species

As underlined into the previous subsection, little is available for Cs-Si-O system thermodynamic properties for the current SA analysis code databases. Regarding Cs-Fe-Si-O system, no data are included. We present hereafter the determination of thermodynamic properties of likely formed Cs chemisorbed species by using first-principles calculations, namely with a DFT based methodology detailed in our previous work [19,20]. As discussed in the Cs chemisorption experiments section, the morphology of Cs chemisorbed species onto the SS surfaces varied with atmosphere and temperature. We focus to the likely formed species in the presence of SS reactor structural materials, under similar conditions to 1-F SA RPV regions, i.e. at the high-temperature range and significant $CsOH_{(g)}$ concentration. Hence, the properties of the following substances are presented:

- $CsFeSiO_4$ and $Cs_2Si_4O_9$, the main characterized Cs chemisorbed species by experiment [5, 6, 10,15,23];
- Cs_2SiO_5 and $Cs_6Si_{10}O_{23}$, possibly formed instead of $Cs_2Si_4O_9$ due to the eutectic transformation feature of these substances at the high-temperature region, as discussed in the previous sub-section;
- $CsFeSi_2O_6$, identified in reductive atmosphere with typical reactor Si content on SS304 specimen [15],
- $Cs_2Fe_2Si_3O_{10}$ theoretically found stable [42] and could be formed in competition with the other Cs-Fe-Si-O substances.

Comparison of the standard enthalpy of formation, entropy and heat capacity of $Cs_2Si_2O_5$ and $Cs_2Si_4O_9$ species allowed assessing the accuracy of our developed DFT methodology [14]. A good agreement was obtained with available literature references, within a relative error of 5 % on average between the calculated and best-estimated literature values (see Table II). No experimental results were reported in the literature for the standard enthalpy of formation, entropy and heat capacity of $CsFeSiO_4$, as well as $CsFe_2SiO_2$, $Cs_6Si_{10}O_{23}$ and $Cs_2Fe_2Si_3O_{10}$. For $CsFeSiO_4$, the thermodynamic properties at low- and high-temperature region determined by DFT are reported in our previous work [19, 20]. In complement to these studies, the accuracy of computed properties will be analyzed by comparing the Raman spectra of $CsFeSiO_4$ with the DFT calculated phonon density of states (PhDOS), which was used to derive the theoretical thermodynamic properties. Then, the thermodynamic properties for the whole Cs-(Fe)-Si-O system are tabulated and discussed in regards to their stability. Finally, application of the constructed Cs chemisorption model to study possible revaporization of $CsFeSiO_4$ is presented.

3.2.1 Vibrational frequencies

To have more insights into the involved vibrational properties of $CsFeSiO_4$ compound (which enter in the calculation of the heat increment, heat capacity and entropy), we compared experimental Raman spectra in Fig.6 with the computed phonon density of states, in Fig.7.

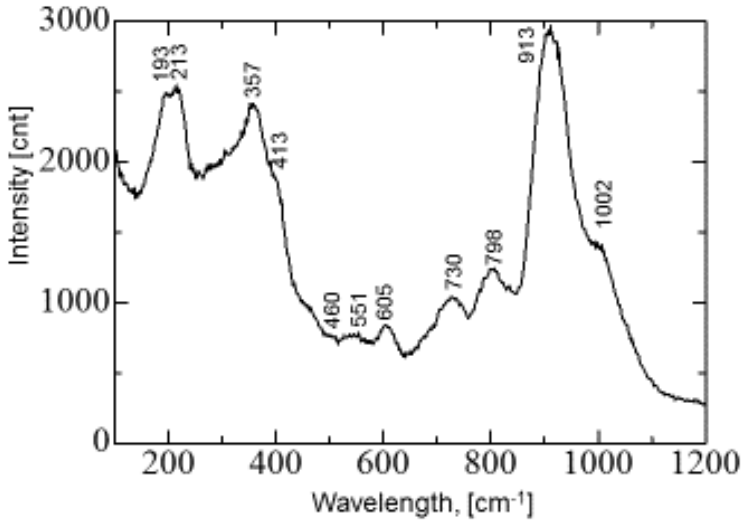

Figure 6. Raman shift of $CsFeSiO_4$ at room temperature [15].

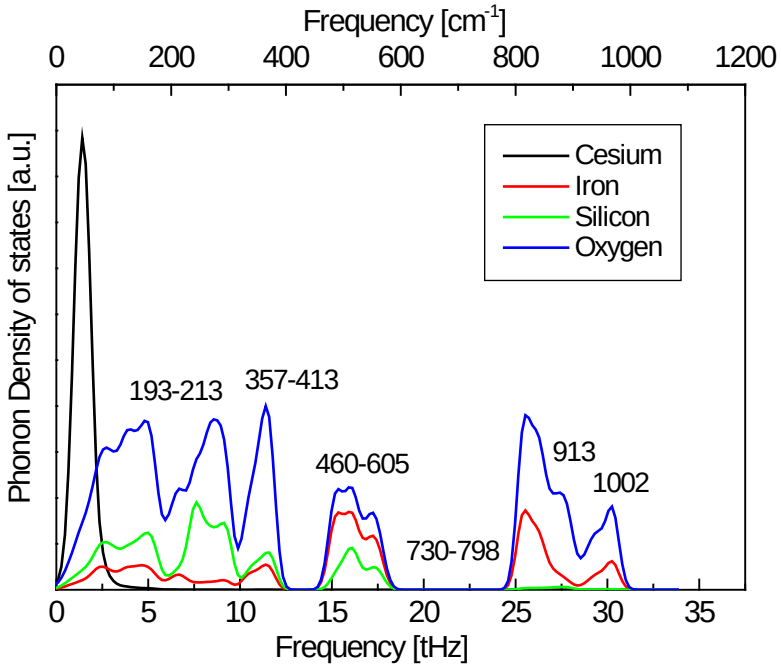

Figure 7. Phonon Density of states calculated for $CsFeSiO_4$.

The vibrational modes referenced in the Raman shifts in Fig. 6 are mainly identified as oxoferrates and oxosilicates stretching and bending modes, in the range of 100 to 1100 cm^{-1}, according to the study of Abassi *et al*. [43] and Shebanova *et al*. [44]. Abassi *et al*. found symmetric (ν_s) and asymmetric (ν_{as}) stretching modes of SiO_4 around 360 and 396-403 cm^{-1}, respectively, which are corroborated onto the PhDOS, displaying larger density for Si-O elements at these frequencies. For the values after 460 cm^{-1}, the phonon frequency curve displays more density for Fe-O elements, translating more vibration from FeO_4 tetrahedron.

The reported values for FeO_4 asymmetric stretching modes by Shebanova *et al.* [41] are c.a. 486-490 cm^{-1}. The symmetric stretching of O atoms along Fe are localized at 625-715 cm^{-1}. Two bending modes of O atoms to Fe are referenced at 306-333cm^{-1} and 538-570 cm^{-1}, respectively for symmetric (δ_s) and asymmetric one (δ_{as}). These modes are associated with almost no movement of Fe atoms that might explain less density of Fe element for δ_s mode displayed into the PhDOS. Finally, a translator movement of the whole FeO_4 ν_{trans} is reported around 193-217cm^{-1} [41]. Peaks at these frequencies could be identified onto the PhDOS, although larger density appeared for Si-O elements. Such result might be explained by a significant broadening and shift feature of SiO_4 bands, generated by the Cs cations disordering for weaker frequencies regions, as discussed by Shebanova and Lazor [44]. As a whole, the determined peaks in the Raman spectra are identified in the PhDOS, affirming the reliability of calculated vibrational frequencies with the DFT approximation.

3.2.2 Thermodynamic properties of Cs-(Fe)-Si-O system

The standard enthalpy of formation, heat capacity, standard entropy and enthalpy increment of Cs chemisorbed species are portrayed in Table II. We reported the heat capacity coefficients for the expansion $C_p(T) = a + bT + cT^2 + dT^{-2}$ in Appendix C. Recently we measured the low-temperature (from 1.9 to 300 K) heat capacity of $Cs_2Si_4O_9$ [22] to obtain a reliable standard entropy for this substance, as the one available in literature was derived from additive rule as described in the previous work [38]. A difference of only 2% was found between the computed heat capacity (253.26 kJ/mol) [14] and the experimental one (248.67 $kJ.mol^{-1}$) [17], as shown in Table II.

Table II. Calculated thermodynamic properties for Cs-(Fe)-Si-O system, comparing with literature. Relative errors are shown in parenthesis with best-estimated literature values in percentage.

Properties	$\Delta_fH_{298.15\,K}$ kJ.mol^{-1}	$H_{298.15\,K}$-H_{0K} kJ.mol^{-1}	$Cp_{298.15\,K}$ J.K^{-1}mol^{-1}	$S_{298.15\,K}$ J.K^{-1}mol^{-1}	[References] Year
Validation of the methodology					
	-2460.9*(1.6)	-	165.18^{*+}(1.0)	229.80^{*+}(4.7)	[32]1973
$Cs_2Si_2O_5$	**-2421.9**	32.05	**163.30**	**240.58**	**DFT**[19]2018
$Cs_2Si_4O_9$	-4341.1*	-	226.9*	313*	[32] 1973
	-4297.6$^{\#}$(4.0)	-	238.99$^{\#}$(5.9)	313*	[38] 1993
	-	45.72$^{\#}$(7.8)	248.67$^{\#}$(1.8)	321$^{\#}$(13.7)	[22] 2018
	-4123.9	**42.73**	**253.26**	**277.07**	**DFT**[19] 2018
Newly obtained thermodynamic properties by this work					
$Cs_2Si_{10}O_{23}$	-10863.9	125.06	670.15	907.95	DFT 2018
$CsFeSiO_4$	-1634.5$^{\$}$(1.2)	-	-	-	DFT [45]2013
	-1659.3	24.62	129.66	177.88	DFT[19] 2018
$CsFeSi_2O_6$	-2567.7	32.09	171.61	235.09	DFT 2018
$Cs_2Fe_2Si_3O_{10}$	-4003.1	56.78	305.13	399.51	DFT 2018

$^{\#}$: derived from experiment, *: estimated value, $^{+}$ updated value, $^{\$}$: DFT calculations at 0 K.

Hence, we could confirm that the theoretical results are in good agreement with available literature data and experiments. It could be noticed that $Cs_2Si_4O_9$ and $Cs_2Si_{10}O_{23}$ present the same standard enthalpy of formation per atom from the DFT calculations (-2.85 and -2.89 eV/atom, respectively). Such result might be explained by the isotype like crystal structures of those both species [19, 46]. As $CsFeSi_2O_6$ was found to be the most stable Cs chemisorbed species in the Cs_2O-SiO_2-Fe_2O_3 system by the DFT calculations [42], it could be of use to perform chemical thermodynamic equilibrium calculations to get the speciation of likely formed Cs chemisorbed species under NPP SA conditions, in particular, those of 1-F SA.

To understand the revaporization phase of likely formed Cs chemisorption species, we provide hereafter a tentative modelling for $CsFeSiO_4$ case, which is the major identified Cs chemisorbed species in our experiments [10,15,23].

3.3. Revaporization phase modelling

The following equation could illustrate the revaporization of Cs chemisorbed species $CsFeSiO_4$:

$$CsFeSiO_4(s) + \frac{3}{2}H_2(g) = CsOH(g) + Fe(s) + SiO_2(s) + H_2O(g) \quad (5)$$

Eq. (3) in section 2.3 presents the revaporization rate N_R for a Cs chemisorbed species, from which the concentration of the chemisorbed species *i* C_{wi} near the surface could be derived in Eq. (4). By applying this equation to Cs chemisorbed species $CsFeSiO_4$, C_{wi} is expressed as follows:

$$C_{wi} = \frac{p(CsOH)}{RT} = \frac{p(H_2)^{\frac{3}{2}}a(CsFeSiO_4)}{p(H_2O)a(Fe)a(SiO_2)} exp\left(\frac{-\Delta_r G^\circ(eq.(5))}{RT}\right)/RT \quad (6)$$

where p is partial pressure, a activity and $\Delta_r G^\circ$ standard reaction Gibbs energy.
The Gibbs energy of the reaction in Eq. 5 could be expressed using the standard free energy of formation of involved species as:

$$\Delta_r G^\circ(\text{eq}(5)) = \Delta_f G^\circ(CsOH, g) + \Delta_f G^\circ(SiO_2, s) + \Delta_f G^\circ(H_2O, g) - \Delta_f G^\circ(CsFeSiO_4, s) \quad (7)$$

The $\Delta_f G^\circ(CsFeSiO_4, s)$ was obtained using the DFT based methodology, the $\Delta_f G^\circ(CsOH, g)$, the $\Delta_f G^\circ(SiO_2, s)$ and the $\Delta_f G^\circ(H_2O, g)$ were taken from the NIST database [44]. Therefore, assuming that all of the $a(Fe)$, the $a(SiO_2)$ and the $a(CsFeSiO_4)$ are equal to unity, we calculated C_{wi} (CsOH concentration at the interface), plotted in Fig 8.

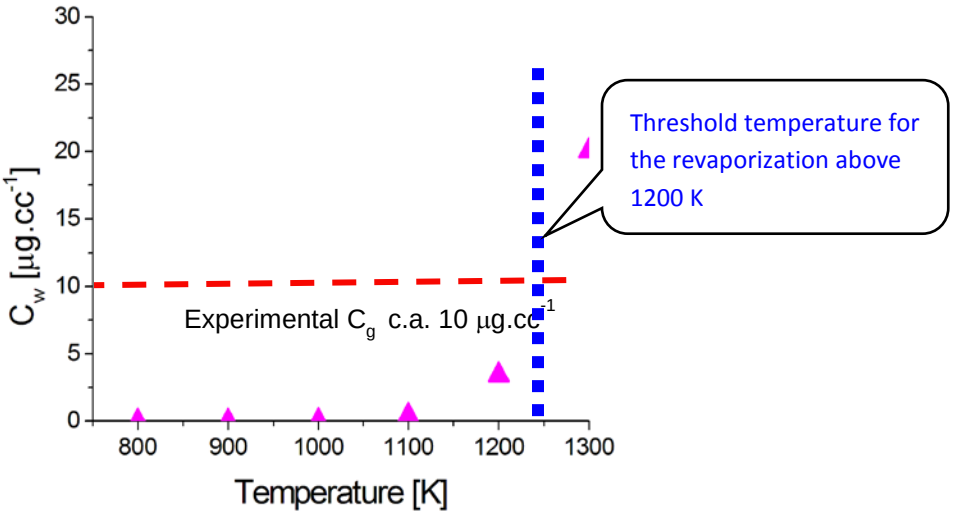

Figure 8. Estimated partial pressure near the gas-solid interface (C_w) in the case of p(H_2)=0.05bar and (H_2O)=0.0005bar.

As our concentration of CsOH for the Cs chemisorption experiment in Ar-H_2 atmosphere was about 10 μg/cc, it seems that the revaporization stage might occur in our reductive atmosphere, confirming the experimental observation.
Theoretical calculations are planned in near future to comprehend the mechanisms involved in the formation of the Cs chemisorbed species, i.e. reaction pathway and diffusion of the Cs particles onto the oxide layers. As discussed in previous sections, the morphology of Cs chemisorbed species might differ significantly within the chemical factors and thus should be reflected by the chemisorption model.

4. CONCLUSIONS

The results for the improvement work of Cs chemisorption model in the SA analysis codes have been reviewed. Related information was also given for the consolidation and extension of knowledge on the thermodynamic properties of the major identified Cs chemisorbed species of the Cs-(Fe)-Si-O system under SA conditions. The main results are listed below.

Our fundamental experimental tests showed that implemented Cs chemisorption models caused uncertainties in the evaluation of Cs distribution by the SA analysis code, mainly due to the lack of incorporated chemical factors like CsOH concentration in the gaseous phase, Si content in stainless steel (SS) surface and atmosphere (H_2/H_2O ratio).

To cover the influence of CsOH concentration and Si content in SS, we developed an improved Cs chemisorption model. The uncertainty caused to the model was greatly reduced by an order of magnitude.

To take the atmospheric composition in the Cs chemisorption process into account, we are currently developing a model to include the revaporization phase of Cs chemisorbed species, mainly Cs-Fe-Si-O substances, by using thermodynamic equilibrium considerations.

A literature survey was accordingly conducted to assess the availability of thermodynamic properties of Cs chemisorbed species and the status of Cs chemisorbed species implemented in the SA analysis code database. It was revealed that consolidation and extension of the thermodynamic properties of the Cs-(Fe)-Si-O system are required.

To elucidate the unknown thermodynamic properties of main identified Cs chemisorbed species of Cs-(Fe)-Si-O system, a DFT based methodology was developed. The calculations revealed not only a good agreement with the existing Cs-Si-O thermodynamic values including our recently performed experimental measurements but also allowed to provide the properties of likely formed species of the Cs-Fe-Si-O system under conditions similar to 1-F SA.

In near future, thermodynamic equilibrium calculations will be performed to assess the speciation regarding the Cs chemisorption onto SS in NPP SA conditions.

ACKNOWLEDGMENTS

The content of this material includes partial output of the METI subsidy for Project of Decommissioning and Contaminated Water Management (upgrading level of grasping state inside reactor).

REFERENCES

1. S. Miwa, S. Yamashita, A. Ishimi, M. Osaka, M. Amaya, K. Tanaka, F. Nagase, "Research Program for the Evaluation of Fission Product and Actinide Release Behaviour, Focusing on their Chemical Forms" *Energy Procedia*, **71**, pp. 168-181 (2015).
2. P.D.W. Bottomley, K. Knebel, S. VanWinckel, T. Haste, S.M.O. Souvi, A. Auvinen, J. Kalilainen, T. Kärkelä, "Revaporisation of fission product deposits in the primary circuit and its impact on accident source term", *Annals of Nucl. Energy*, **74**, pp. 208-223 (2014).
3. Nuclear Damage Compensation and Decommissioning Facilitation Corporation decommissioning office (NDF), "Technical strategic plan 2016 for decommissioning of the Fukushima Daiichi Nuclear Power Station of Tokyo Electric Power Company holdings Inc." pp.4-38 (2016).
4. V.F. Baston, , K.J. Hofstetter, G.M. Bain, R.M. Elrick, "A comparison of TMI-2 and laboratory results for cesium activity retained on reactor material surfaces", *American Nuclear Society Winter Meeting San Francisco*, California, November 10-14, 1985, pp. 223-225 (1985).
5. R.M. Elrick, R.A Sallach, A.L. Ouellette, S.C Douglas, "Reaction between some cesium-iodine compounds and the reactor materials 304 stainless steel, inconel 600 and silver", NUREG/CR-3197 vol. 1, SAND83-0395 (1984).
6. R.M. Elrick and D. A. Powers, "High-temperature fission-product chemistry and transport", U.S. nuclear regulatory commission, reactor safety research semiannual report, July- December, 1986 volume 36, NUREG/CR-4805 (2 of 2), SAND86-2752 (2 of 2) (1987).
7. B.R. Bowsher, S. Dickinson, A.L. Nichols, "High temperature studies of simulant fission products: part III, Temperature-dependent interaction of cesium hydroxide vapor with 304 stainless steel", AEEW-R 1863, Technology division, AEE Winfrith (1990).
8. I. Johnson, M.K. Farahat, J. L Settle, J. D. Arntzen, C. E. Johnson, "Downstream behavior of volatile iodine, cesium, and tellurium fission products", EPRI NP-6182 Research project 2136-1 Final report, January (1989).
9. D. Cubicciotti, B. R. Sehgal, "Vapor Transport of Fission Products in Postulated Severe Light Water Reactor Accidents", *Nucl. Tech*., **65**, pp 266-291, (1984).
10. F.G. Di Lemma, K. Nakajima, S. Yamashita, M. Osaka, "Experimental investigation of the influence of Mo contained in stainless steel on Cs chemisorption behavior", *J. Nucl. Mat*., **484**, pp. 174-182 (2017).
11. M.Yamawaki, T. Oka, M. Yasumoto, H. Sakurai, "Thermodynamics of vaporization of cesium molybdate by means of mass spectrometry" *J Nucl. Mat.*, **201**, pp. 257-260 (1993).
12. M. Plys, S.J. Lee, R. Apthorpe, "Review of Japanese Core Team Cesium Chemistry Model", JFY2016 Task. FAI/16-1416, Rev. 1, EPRI 3002009886 (2017).
13. M. Osaka, K. Nakajima, S. Miwa, F.G.Di Lemma, N. Miyahara, C. Suzuki, E. Suzuki, T. Okane, M. Kobata, "Results and Progress of Fundamental Research on FP Chemistry", *Proceedings of the 8th European Review Meeting on Severe Accident Research-ERMSAR-2017*, Warsaw, Poland, May 16 -18 (2017).
14. S. Nishioka, K. Nakajima, E. Suzuki, M. Osaka, "Experimental investigation of influencing factors on Cs chemisorption behavior onto stainless steel", *J. Nucl. Mater.*, to be submitted (2018).
15. F.G. Di Lemma, K. Nakajima, S. Yamashita, M. Osaka, "Surface analyses of cesium hydroxide chemisorbed onto type 304 stainless steel", *Nucl. Eng. Des.*, **305**, pp. 411-420 (2016).
16. A. S. Mamede et al., "Multitechnique characterisation of 304L surface states oxidised at high temperature in steam and air atmospheres" *Applied Surf. Sci.*, **369**, pp.510-519,(2016).
17. K. Nakajima, S. Nishioka, E. Suzuki, M. Osaka, "Study on chemisorption model of cesium hydroxide onto stainless steel type 304", *27th International Conference on Nuclear Engineering.(ICONE27)*, to be submitted (2018).
18. Thermodynamic Mephista Database, Institut de Radioprotection et Sûreté Nucléaire (IRSN), F-13115 St Paul lez Durance (France)
19. F. Miradji, C. Suzuki, K. Nakajima, M. Osaka, "Cesium chemisorbed species onto stainless steel surfaces: an atomistic scale study", *submitted to J. Phys. Chem. Solids* (2018).

20. F. Miradji, C. Suzuki, E. Suzuki, S. Nishioka, K. Nakajima, M. Osaka, "Structural, electronic and thermodynamic properties of cesium chemisorbed species onto stainless steel", *submitted to J. Alloy. and Compd*., **VSI-HTMC16** (2018).
21. T. M. D. Do, K. Murakami, M. Suzuki, M. Osaka, "Raman spectra of cesium iron silicate", *Atomic Energy Society of Japan 2018 Annual Meeting*, Osaka University Suita Campus, Japan, (2018).
22. E. Suzuki, K. Nakajima, M. Osaka, Y. Ohishi, H. Muta, K. Kurosaki, "Low temperature heat capacity of $Cs_2Si_4O_9$", *subjected to J. Alloy. and Compd*., **VSI-HTMC16** (2018).
23. M. Kobata, T. Okane, K. Nakajima, E. Suzuki, K. Ohwada, K. Kobayashi, H. Yamagami, M. Osaka, "Chemical form analysis of reaction products in Cs-adsorption on stainless steel by means of HAXPES and SEM/EDX", *J. Nucl. Mat.*, **498**, pp. 387-394 (2018).
24. G. C. Allen, B. R. Bowsher, S. Dickinson, G. M. Fotios, A. L. Nichols, R. K. Wild, "Surface studies of the interaction of cesium hydroxide vapor with 304 stainless steel" *Oxidation of Metals*, **28** (1), pp 33-59 (1987).
25. T.S. Sherwood, T.S., R.L Pigford, C.R. Wilke, *Mass transfer*, pp. 80/153-155/178-181/312-320, McGraw-Hill, New-York (1975).
26. C. Hoch, C. Rohr, "The alkaline metal oxo-silicates A6[Si309] and A6[Si207] (A = Rb, Cs): preparation and crystal ctructure", *Z. Naturforschg.* **56** B, pp. 423-430 (2001).
27. V. Hlukky, T.F. Fassler, "The new alkali cyclotrisilicate Cs8[Si6O16]", *Z. Anorg. Allg. Chem*. **639** pp. 231-233 (2013).
28. B.H.W.S. De Jong, P.G.G. Slaats, H.T.J. Super, N. Veldman, A.L. Spek, "Extended structures in crystalline phyllosilicates: silica ring systems in lithium, rubidium, cesium, and cesium/lithium phyllosilicate", J. *of Non-Cryst. Solids* **176**(2), pp. 164-171 (1994).
29. A.E. Lapshin, N.V. Borisova, V.M. Ushakov, Y.F. Shepelev, "Crystal structure and some thermodynamic characteristics of cesium cilicate $Cs_6Si_{10}O_{23}$", *Russian J. of Inorg. Chemi.*, **51**(11), pp. 1696-1700 (2006).
30. A.E. Lapshin, N.V. Borisova, V.M. Ushakov, Y.F. Shepelev, "Disordering in the structure of cesium silicate $Cs_6Si_{10}O_{23}$", *Glass Phys. and Chem.*, **33**(3), pp. 250-253 (2007).
31. S. Hoffmann, T.F. Fassler, C. Hoch, C. Rohr, C., Alkali metal tetrelide–tetrelates: "Double salts With [E4]4-; zintl anions (E=Si, Ge) and the first dimeric cyclotrisilicate ions [Si6O17]10-", *Angew. Chem. Int. Ed. Engl*., **40** (23), pp. 4398-4400 (2001).
32. P.J. Spencer, *The thermodynamic properties of pilicates*, NPL Report Chem. 21, (1973).
33. Z.D. Alekseeva, "The Cs2O-SiO2 system", *Russian J. Inorg. Chem.*, **11**(5), pp. 626-629 (1966)
34. P. Boivin, J.C. Berthelay, Y. Blanc, A. Coulet, R. Castanet, "Determination of temperature and enthalpy of melting of alkali disilicates by differential calorimetric analysis", *J. Mater. Sci.*, **28**, pp. 1834-1838 (1993).
35. F. Bennour, *Contribution à l'Etude Thermodynamique des Silicates Liquides-Système Cs_2O-SiO_2-Na_2O*, PhD Thesis, Aix-Marseille University, (1995).
36. F. Bennour, J. Rogez, J.C. Mathieu, "Phase equilibria in the Na_2O-Cs_2O-SiO_2 system", *J. Am. Ceram. Soc.*, **79** (10), 2752-2754 (1996).
37. E.H.P. Cordfunke, W. Ouweltjes, "The standard molar enthalpies of formation of Cs_2MnO_4, $Cs2Si_4O_9$, and Cs_3PO_4 ", *J. Chem. Thermodyn.*, **25** (8), pp. 1011-1016 (1993).
38. R.G.J. Ball, B.R. Bowsher, E.H.P. Cordfunke, S. Dickinson, R.J.M. Konings, "Thermochemistry of selected fission product compounds", *J. Nucl. Mater.*, **201**, pp. 81-91 (1993).
39. R.J. Charles, "Metastable liquid immiscibility in alkali metal oxide-silica systems", *J. Am. Ceram, Soc,*, **49** (2), pp. 55-62 (1966).
40. M. Morishita, A. Navrotsky, M.C. Wilding, "Direct measurement of relative partial molar enthalpy of SiO_2 in SiO_2–M_2O (M=Li, Na, K, Cs) Binary and SiO_2–CaO–Al_2O_3 ternary melts", *J. Am. Ceram, Soc*., **87** (8), pp.1550-1555 (2004).
41. E. Fischer, Private communication (2018).
42. C. Suzuki., K. Nakajima, M. Osaka, "Phase stability of Cs-Si-O and Cs-Si-Fe-O compounds on stainless steel", *J. Nucl.Sci. and Tech*., to be submitted (2018).

43. M. Abbassi, R. Ternane, I. Sobrados, A. Madani, M. Trabelsi-Ayadi, J. Sanz, "Synthesis, characterization and oxide conduction in Ba doped apatite-type silicates Ca2La6Bi2(SiO4)6O2", *Mater. Chem. and Phys.*, **147** (1–2), pp. 285-292 (2014).
44. O. n. Shebanova and P. Lazor, "Raman study of magnetite (Fe3O4): laser‐induced thermal effects and oxidation", *J. Raman Spectrosc*., **34**, pp 845-852 (2003).
45. J. Saal, S. Kirklin, M. E. A. Aykol, *JOM* **65**, pp. 1501 (2013).
46. H. Schichl, H. Völlenkle, A. Wittmann, "Die Kristallstructur von Rb6Si10O23", *Monatshefte für Chemie* **104**, pp. 854-863 (1973).
47. M. W. Chase, "NIST-JANAF thermochemical tables fourth edition Part I, Al – Co, Part II, Cr-Zr", Jr., J. Phys. Chem. Ref. Data, Monograph No. 9, (1998).

APPENDIX A

Figure A. Dependence of surface reaction rate constant v_d on Si content in SS304 specimen. (a) water-soluble Cs compounds; (b) water-insoluble Cs compounds. From Nishioka et al. [14]. The average deviation of v_d is ±34,7%.

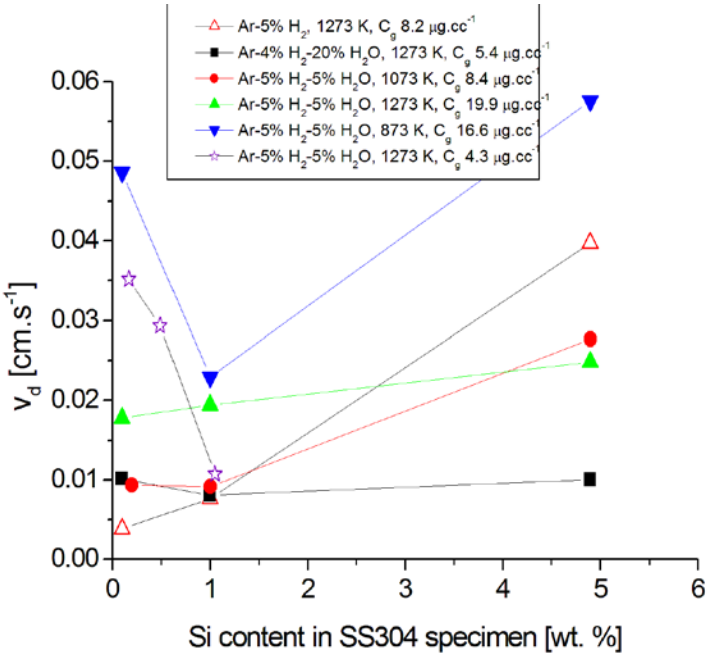

(a) water-soluble Cs.

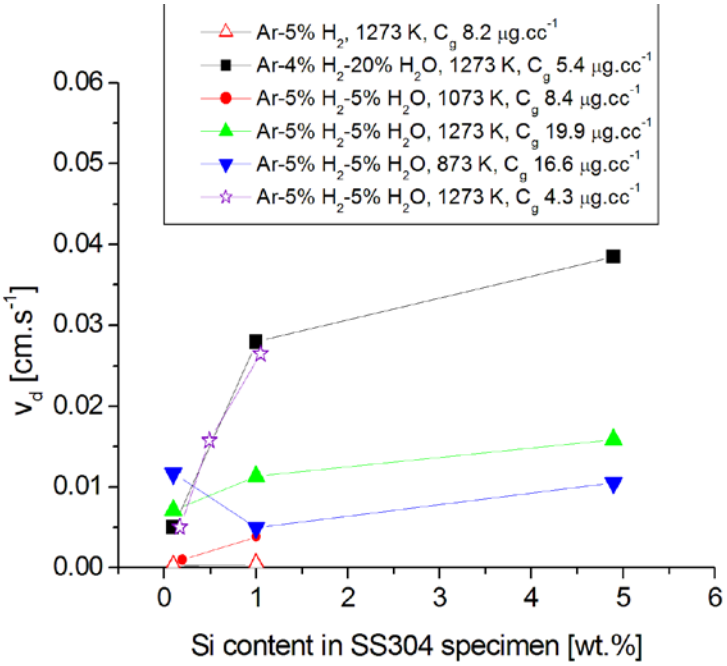

(b) water-insoluble Cs.

APPENDIX B

Figure B. Dependence of surface reaction rate constant v_d on CsOH concentration in the gaseous phase (C_g) in H_2O-containing atmosphere. (a) water-soluble Cs compounds; (b) water-insoluble Cs compounds. From Nishioka et al. [14]. The average deviation of v_d is ±34,7%

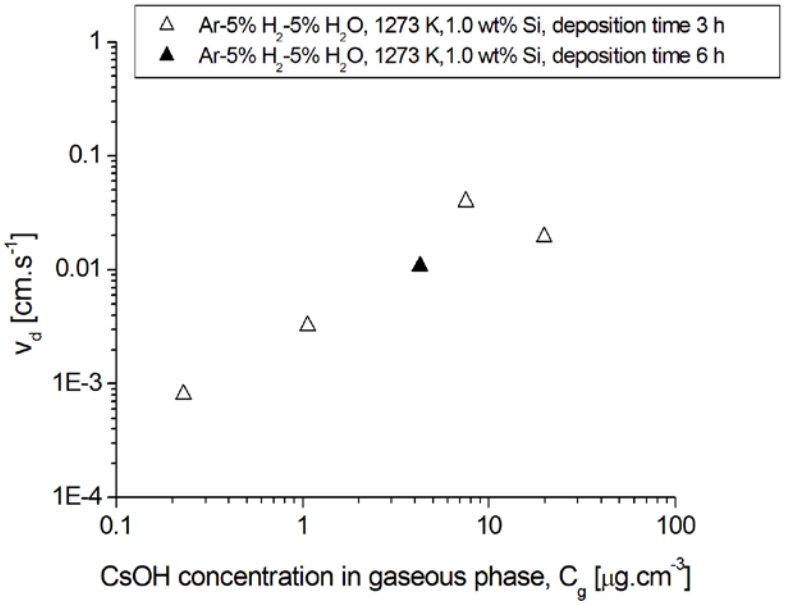

(a) water-soluble Cs.

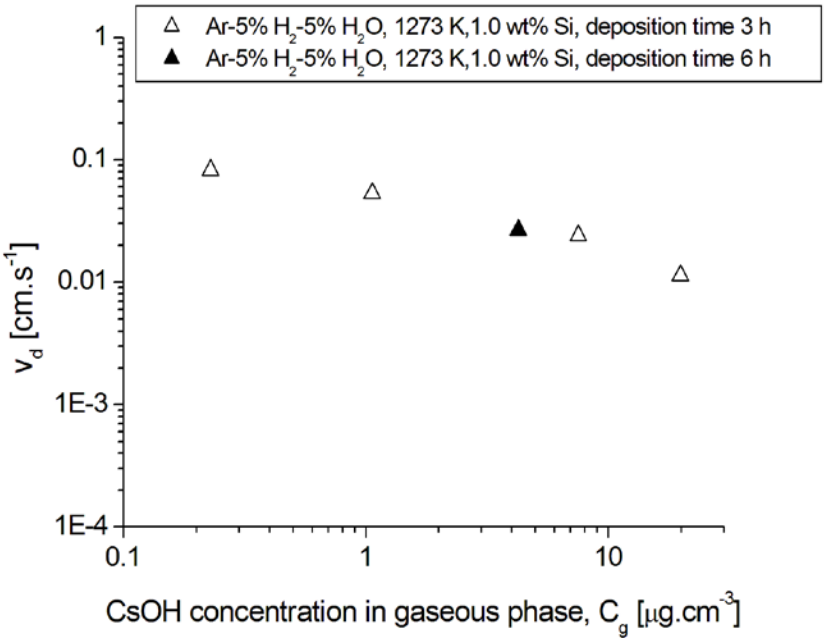

(b) **water-insoluble Cs compounds.**

APPENDIX C

Table C. Heat capacity coefficients for the expansion $C_p(T) = a + bT + cT^2 + dT^{-2}$ computed within DFT theory for Cs-(Fe)-Si-O substances

Substances	T range (K)	a $J.K^{-1}mol^{-1}$	b $J.K^{-2}mol^{-1}$	c $J.K^{-3}mol^{-1}$	d $J.K\,mol^{-1}$
$Cs_2Si_2O_5$	298-1000	1.639E+02	1.015E-01	-4.863E-05	-2.410E+06
$Cs_2Si_4O_9$	298-1000	2.653E+02	1.840E-01	-8.868E-05	-5.344E+06
$Cs_6Si_{10}O_{23}$	298-1000	6.640E+02	5.153E-01	-2.462E-04	-1.141E+07
$CsFeSiO_4$	298-1000	1.336E+02	8.513E-02	-4.316E-05	-2.025E+06
$CsFeSi_2O_6$	298-1000	1.745E+02	1.208E-01	-5.807E-05	-3.060E+06
$Cs_2Fe_2Si_3O_{10}$	298-1000	3.213E+02	1.740E-01	-8.433E-05	-5.479E+06